PHYSICAL REVIEW D **89,** 071101(R) (2014)

Search for the rare decays $J/\psi \to D_s^- \rho^+$ and $J/\psi \to \bar{D}^0 \bar{K}^{*0}$

M. Ablikim,[1] M. N. Achasov,[8,†] X. C. Ai,[1] O. Albayrak,[4] M. Albrecht,[3] D. J. Ambrose,[41] F. F. An,[1] Q. An,[42] J. Z. Bai,[1] R. Baldini Ferroli,[19a] Y. Ban,[28] J. V. Bennett,[18] M. Bertani,[19a] J. M. Bian,[40] E. Boger,[21,‡] O. Bondarenko,[22] I. Boyko,[21] S. Braun,[37] R. A. Briere,[4] H. Cai,[47] X. Cai,[1] O. Cakir,[36a] A. Calcaterra,[19a] G. F. Cao,[1] S. A. Cetin,[36b] J. F. Chang,[1] G. Chelkov,[21,‡] G. Chen,[1] H. S. Chen,[1] J. C. Chen,[1] M. L. Chen,[1] S. J. Chen,[26] X. Chen,[1] X. R. Chen,[23] Y. B. Chen,[1] H. P. Cheng,[16] X. K. Chu,[28] Y. P. Chu,[1] D. Cronin-Hennessy,[40] H. L. Dai,[1] J. P. Dai,[1] D. Dedovich,[21] Z. Y. Deng,[1] A. Denig,[20] I. Denysenko,[21] M. Destefanis,[45a,45c] W. M. Ding,[30] Y. Ding,[24] C. Dong,[27] J. Dong,[1] L. Y. Dong,[1] M. Y. Dong,[1] S. X. Du,[49] J. Z. Fan,[35] J. Fang,[1] S. S. Fang,[1] Y. Fang,[1] L. Fava,[45b,45c] C. Q. Feng,[42] C. D. Fu,[1] O. Fuks,[21,‡] Q. Gao,[1] Y. Gao,[35] C. Geng,[42] K. Goetzen,[9] W. X. Gong,[1] W. Gradl,[20] M. Greco,[45a,45c] M. H. Gu,[1] Y. T. Gu,[11] Y. H. Guan,[1] A. Q. Guo,[27] L. B. Guo,[25] T. Guo,[25] Y. P. Guo,[20] Y. L. Han,[1] F. A. Harris,[39] K. L. He,[1] M. He,[1] Z. Y. He,[27] T. Held,[3] Y. K. Heng,[1] Z. L. Hou,[1] C. Hu,[25] H. M. Hu,[1] J. F. Hu,[37] T. Hu,[1] G. M. Huang,[5] G. S. Huang,[42] H. P. Huang,[47] J. S. Huang,[14] L. Huang,[1] X. T. Huang,[30] Y. Huang,[26] T. Hussain,[44] C. S. Ji,[42] Q. Ji,[1] Q. P. Ji,[27] X. B. Ji,[1] X. L. Ji,[1] L. L. Jiang,[1] L. W. Jiang,[47] X. S. Jiang,[1] J. B. Jiao,[30] Z. Jiao,[16] D. P. Jin,[1] S. Jin,[1] T. Johansson,[46] N. Kalantar-Nayestanaki,[22] X. L. Kang,[1] X. S. Kang,[27] M. Kavatsyuk,[22] B. Kloss,[20] B. Kopf,[3] M. Kornicer,[39] W. Kuehn,[37] A. Kupsc,[46] W. Lai,[1] J. S. Lange,[37] M. Lara,[18] P. Larin,[13] M. Leyhe,[3] C. H. Li,[1] Cheng Li,[42] Cui Li,[42] D. Li,[17] D. M. Li,[49] F. Li,[1] G. Li,[1] H. B. Li,[1] J. C. Li,[1] K. Li,[30] K. Li,[12] Lei Li,[1] P. R. Li,[38] Q. J. Li,[1] T. Li,[30] W. D. Li,[1] W. G. Li,[1] X. L. Li,[30] X. N. Li,[1] X. Q. Li,[27] Z. B. Li,[34] H. Liang,[42] Y. F. Liang,[32] Y. T. Liang,[37] D. X. Lin,[13] B. J. Liu,[1] C. L. Liu,[4] C. X. Liu,[1] F. H. Liu,[31] Fang Liu,[1] Feng Liu,[5] H. B. Liu,[11] H. H. Liu,[15] H. M. Liu,[1] J. Liu,[1] J. P. Liu,[47] K. Liu,[35] K. Y. Liu,[24] P. L. Liu,[30] Q. Liu,[38] S. B. Liu,[42] X. Liu,[23] Y. B. Liu,[27] Z. A. Liu,[1] Zhiqiang Liu,[1] Zhiqing Liu,[20] H. Loehner,[22] X. C. Lou,[1,§] G. R. Lu,[14] H. J. Lu,[16] H. L. Lu,[1] J. G. Lu,[1] X. R. Lu,[38] Y. Lu,[1] Y. P. Lu,[1] C. L. Luo,[25] M. X. Luo,[48] T. Luo,[39] X. L. Luo,[1] M. Lv,[1] F. C. Ma,[24] H. L. Ma,[1] Q. M. Ma,[1] S. Ma,[1] T. Ma,[1] X. Y. Ma,[1] F. E. Maas,[13] M. Maggiora,[45a,45c] Q. A. Malik,[44] Y. J. Mao,[28] Z. P. Mao,[1] J. G. Messchendorp,[22] J. Min,[1] T. J. Min,[1] R. E. Mitchell,[18] X. H. Mo,[1] Y. J. Mo,[5] H. Moeini,[22] C. Morales Morales,[13] K. Moriya,[18] N. Yu. Muchnoi,[8,†] H. Muramatsu,[40] Y. Nefedov,[21] I. B. Nikolaev,[8,†] Z. Ning,[1] S. Nisar,[7] X. Y. Niu,[1] S. L. Olsen,[29] Q. Ouyang,[1] S. Pacetti,[19b] M. Pelizaeus,[3] H. P. Peng,[42] K. Peters,[9] J. L. Ping,[25] R. G. Ping,[1] R. Poling,[40] N. Q.,[47] M. Qi,[26] S. Qian,[1] C. F. Qiao,[38] L. Q. Qin,[30] X. S. Qin,[1] Y. Qin,[28] Z. H. Qin,[1] J. F. Qiu,[1] K. H. Rashid,[44] C. F. Redmer,[20] M. Ripka,[20] G. Rong,[1] X. D. Ruan,[11] A. Sarantsev,[21,‖] K. Schoenning,[46] S. Schumann,[20] W. Shan,[28] M. Shao,[42] C. P. Shen,[2] X. Y. Shen,[1] H. Y. Sheng,[1] M. R. Shepherd,[18] W. M. Song,[1] X. Y. Song,[1] S. Spataro,[45a,45c] B. Spruck,[37] G. X. Sun,[1] J. F. Sun,[14] S. S. Sun,[1] Y. J. Sun,[42] Y. Z. Sun,[1] Z. J. Sun,[1] Z. T. Sun,[42] C. J. Tang,[32] X. Tang,[1] I. Tapan,[36c] E. H. Thorndike,[41] D. Toth,[40] M. Ullrich,[37] I. Uman,[36b] G. S. Varner,[39] B. Wang,[27] D. Wang,[28] D. Y. Wang,[28] K. Wang,[1] L. L. Wang,[1] L. S. Wang,[1] M. Wang,[30] P. Wang,[1] P. L. Wang,[1] Q. J. Wang,[1] S. G. Wang,[28] W. Wang,[1] X. F. Wang,[35] Y. D. Wang,[19a] Y. F. Wang,[1] Y. Q. Wang,[20] Z. Wang,[1] Z. G. Wang,[1] Z. H. Wang,[42] Z. Y. Wang,[1] D. H. Wei,[10] J. B. Wei,[28] P. Weidenkaff,[20] S. P. Wen,[1] M. Werner,[37] U. Wiedner,[3] M. Wolke,[46] L. H. Wu,[1] N. Wu,[1] Z. Wu,[1] L. G. Xia,[35] Y. Xia,[17] D. Xiao,[1] Z. J. Xiao,[25] Y. G. Xie,[1] Q. L. Xiu,[1] G. F. Xu,[1] L. Xu,[1] Q. J. Xu,[12] Q. N. Xu,[38] X. P. Xu,[33] Z. Xue,[1] L. Yan,[42] W. B. Yan,[42] W. C. Yan,[42] Y. H. Yan,[17] H. X. Yang,[1] L. Yang,[47] Y. Yang,[5] Y. X. Yang,[10] H. Ye,[1] M. Ye,[1] M. H. Ye,[6] B. X. Yu,[1] C. X. Yu,[27] H. W. Yu,[28] J. S. Yu,[23] S. P. Yu,[30] C. Z. Yuan,[1] W. L. Yuan,[26,*] Y. Yuan,[1] A. Yuncu,[36b] A. A. Zafar,[44] A. Zallo,[19a] S. L. Zang,[26] Y. Zeng,[17] B. X. Zhang,[1] B. Y. Zhang,[1] C. Zhang,[26] C. B. Zhang,[17] C. C. Zhang,[1] D. H. Zhang,[1] H. H. Zhang,[34] H. Y. Zhang,[1] J. J. Zhang,[1] J. Q. Zhang,[1] J. W. Zhang,[1] J. Y. Zhang,[1] J. Z. Zhang,[1] S. H. Zhang,[1] X. J. Zhang,[1] X. Y. Zhang,[30] Y. Zhang,[1] Y. H. Zhang,[1] Z. H. Zhang,[5] Z. P. Zhang,[42] Z. Y. Zhang,[47] G. Zhao,[1] J. W. Zhao,[1] Lei Zhao,[42] Ling Zhao,[1] M. G. Zhao,[27] Q. Zhao,[1] Q. W. Zhao,[1] S. J. Zhao,[49] T. C. Zhao,[1] X. H. Zhao,[26] Y. B. Zhao,[1] Z. G. Zhao,[42] A. Zhemchugov,[21,‡] B. Zheng,[43] J. P. Zheng,[1] Y. H. Zheng,[38] B. Zhong,[25] L. Zhou,[1] Li Zhou,[27] X. Zhou,[47] X. K. Zhou,[38] X. R. Zhou,[42] X. Y. Zhou,[1] K. Zhu,[1] K. J. Zhu,[1] X. L. Zhu,[35] Y. C. Zhu,[42] Y. S. Zhu,[1] Z. A. Zhu,[1] J. Zhuang,[1] B. S. Zou,[1] and J. H. Zou[1]

(BESIII Collaboration)

[1]*Institute of High Energy Physics, Beijing 100049, People's Republic of China*
[2]*Beihang University, Beijing 100191, People's Republic of China*
[3]*Bochum Ruhr-University, D-44780 Bochum, Germany*
[4]*Carnegie Mellon University, Pittsburgh, Pennsylvania 15213, USA*
[5]*Central China Normal University, Wuhan 430079, People's Republic of China*
[6]*China Center of Advanced Science and Technology, Beijing 100190, People's Republic of China*
[7]*COMSATS Institute of Information Technology, Lahore, Defence Road, Off Raiwind Road, 54000 Lahore*
[8]*G.I. Budker Institute of Nuclear Physics SB RAS (BINP), Novosibirsk 630090, Russia*
[9]*GSI Helmholtzcentre for Heavy Ion Research GmbH, D-64291 Darmstadt, Germany*
[10]*Guangxi Normal University, Guilin 541004, People's Republic of China*
[11]*GuangXi University, Nanning 530004, People's Republic of China*

[12]*Hangzhou Normal University, Hangzhou 310036, People's Republic of China*
[13]*Helmholtz Institute Mainz, Johann-Joachim-Becher-Weg 45, D-55099 Mainz, Germany*
[14]*Henan Normal University, Xinxiang 453007, People's Republic of China*
[15]*Henan University of Science and Technology, Luoyang 471003, People's Republic of China*
[16]*Huangshan College, Huangshan 245000, People's Republic of China*
[17]*Hunan University, Changsha 410082, People's Republic of China*
[18]*Indiana University, Bloomington, Indiana 47405, USA*
[19a]*INFN Laboratori Nazionali di Frascati, I-00044 Frascati, Italy*
[19b]*INFN and University of Perugia, I-06100 Perugia, Italy*
[20]*Johannes Gutenberg University of Mainz, Johann-Joachim-Becher-Weg 45, D-55099 Mainz, Germany*
[21]*Joint Institute for Nuclear Research, 141980 Dubna, Moscow region, Russia*
[22]*KVI, University of Groningen, NL-9747 AA Groningen, The Netherlands*
[23]*Lanzhou University, Lanzhou 730000, People's Republic of China*
[24]*Liaoning University, Shenyang 110036, People's Republic of China*
[25]*Nanjing Normal University, Nanjing 210023, People's Republic of China*
[26]*Nanjing University, Nanjing 210093, People's Republic of China*
[27]*Nankai university, Tianjin 300071, People's Republic of China*
[28]*Peking University, Beijing 100871, People's Republic of China*
[29]*Seoul National University, Seoul 151-747, Korea*
[30]*Shandong University, Jinan 250100, People's Republic of China*
[31]*Shanxi University, Taiyuan 030006, People's Republic of China*
[32]*Sichuan University, Chengdu 610064, People's Republic of China*
[33]*Soochow University, Suzhou 215006, People's Republic of China*
[34]*Sun Yat-Sen University, Guangzhou 510275, People's Republic of China*
[35]*Tsinghua University, Beijing 100084, People's Republic of China*
[36a]*Ankara University, Dogol Caddesi, 06100 Tandogan, Ankara, Turkey*
[36b]*Dogus University, 34722 Istanbul, Turkey*
[36c]*Uludag University, 16059 Bursa, Turkey*
[37]*Universitaet Giessen, D-35392 Giessen, Germany*
[38]*University of Chinese Academy of Sciences, Beijing 100049, People's Republic of China*
[39]*University of Hawaii, Honolulu, Hawaii 96822, USA*
[40]*University of Minnesota, Minneapolis, Minnesota 55455, USA*
[41]*University of Rochester, Rochester, New York 14627, USA*
[42]*University of Science and Technology of China, Hefei 230026, People's Republic of China*
[43]*University of South China, Hengyang 421001, People's Republic of China*
[44]*University of the Punjab, Lahore 54590, Pakistan*
[45a]*University of Turin, I-10125 Turin, Italy*
[45b]*University of Eastern Piedmont, I-15121 Alessandria, Italy*
[45c]*INFN, I-10125 Turin, Italy*
[46]*Uppsala University, Box 516, SE-75120 Uppsala, Sweden*
[47]*Wuhan University, Wuhan 430072, People's Republic of China*
[48]*Zhejiang University, Hangzhou 310027, People's Republic of China*
[49]*Zhengzhou University, Zhengzhou 450001, People's Republic of China*

(Received 17 February 2014; published 9 April 2014)

A search for the rare decays of $J/\psi \to D_s^- \rho^+ + \text{c.c.}$ and $J/\psi \to \bar{D}^0 \bar{K}^{*0} + \text{c.c.}$ is performed with a data sample of 225.3-million J/ψ events collected with the Beijing Spectrometer III detector. No evident signal is observed. Upper limits on the branching fractions are determined to be $\mathcal{B}(J/\psi \to D_s^- \rho^+ + \text{c.c.}) < 1.3 \times 10^{-5}$ and $\mathcal{B}(J/\psi \to \bar{D}^0 \bar{K}^{*0} + \text{c.c.}) < 2.5 \times 10^{-6}$ at the 90% confidence level.

DOI: 10.1103/PhysRevD.89.071101 PACS numbers: 13.25.Gv, 12.60.-i, 14.40.Lb

I. INTRODUCTION

The decays of the low-lying charmonium state J/ψ, which is below the open-charm threshold, are dominated by strong interactions through intermediate gluons and electromagnetic interactions through virtual photons, where both the intermediate gluons and photons are produced by $c\bar{c}$ annihilation. However, flavor-changing

*yuanwl@ihep.ac.cn
†Also at the Novosibirsk State University, Novosibirsk 630090, Russia.
‡Also at the Moscow Institute of Physics and Technology, Moscow 141700, Russia.
§Also at University of Texas at Dallas, Richardson, Texas 75083, USA.
‖Also at the PNPI, Gatchina 188300, Russia.

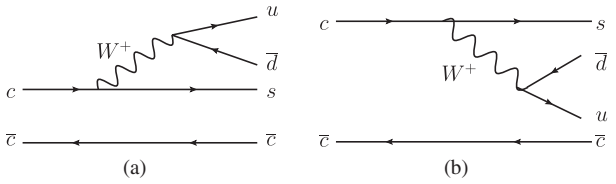

FIG. 1. Leading-order Feynman diagrams for (a) $J/\psi \to D_s^- \rho^+$ and (b) $J/\psi \to \bar{D}^0 \bar{K}^{*0}$.

weak decays of J/ψ through virtual intermediate bosons are also possible in the standard model (SM) framework, and the branching fractions of J/ψ inclusive weak decays are estimated to be on the order of 10^{-8} [1]. Several models addressing new physics, including the top-color model, the minimal supersymmetric standard model (MSSM) with R-parity violation and a general two-Higgs doublet model (2HDM), allow J/ψ flavor-changing processes to occur with branching fractions around 10^{-5}, which may be measurable in experiments [2,3]. Searches for rare J/ψ decays to a single charmed meson provide an experimental test of the SM and a way to look for possible new physics beyond the SM.

The BESII experiment has searched for semileptonic decays and hadronic decays of $J/\psi \to D_s^- \pi^+$, $J/\psi \to D^- \pi^+$, and $J/\psi \to \bar{D}^0 \bar{K}^0$ [4] and set upper limits on the order of $10^{-4} \sim 10^{-5}$ using a sample of 5.8×10^7 J/ψ events [5,6]. With the prospect of high-statistics J/ψ samples, theoretical calculations of the branching fractions of two-body hadronic weak decays of $J/\psi \to DP/DV$, where D represents a charmed meson and P and V the pseudoscalar and vector mesons, respectively, have been performed [7–12]. The branching fractions of $J/\psi \to D_s^- \rho^+$ and $J/\psi \to \bar{D}^0 \bar{K}^{*0}$ are predicted to be higher than those of $J/\psi \to D_s^- \pi^+$ and $J/\psi \to \bar{D}^0 \bar{K}^0$, e.g., the relative ratio $\mathcal{B}(J/\psi \to D_s^- \rho^+)/\mathcal{B}(J/\psi \to D_s^- \pi^+) = 4.2$ [12].

In this analysis, we search for two Cabibbo-favored decay modes $J/\psi \to D_s^- \rho^+$ [Fig. 1(a)] and $J/\psi \to \bar{D}^0 \bar{K}^{*0}$ [Fig. 1(b)] based on $(225.3 \pm 2.8) \times 10^6$ J/ψ events [13] accumulated with the Beijing Spectrometer III (BESIII) detector [14], located at the Beijing Electron-Positron Collider (BEPCII) [15].

II. THE BESIII EXPERIMENT AND MONTE CARLO SIMULATION

The BESIII detector with a geometrical acceptance of 93% of 4π, consists of a small-celled, helium-based main drift chamber (MDC), an electromagnetic calorimeter (EMC) made of CsI(Tl) crystals, a plastic scintillator time-of-flight system (TOF), a superconducting solenoid magnet, and a muon chamber system (MUC) made of resistive plate chambers. The detector has been described in detail elsewhere [14].

The optimization of the event selection and the estimation of physics backgrounds are performed using Monte Carlo (MC)-simulated data samples. The GEANT4-based simulation software BOOST [16] includes the geometric and material description of the BESIII detectors and the detector response and digitization models, as well as the tracking of the detector running conditions and performance. The production of the J/ψ resonance is simulated by the MC event generator KKMC [17]; the known decay modes are generated by EVTGEN [18] with branching fractions set at world average values [19], while the remaining unknown decay modes are modeled by LUNDCHARM [20].

III. DATA ANALYSIS

In order to avoid large background contamination from conventional J/ψ hadronic decays, the D_s^- and $\bar{D}^0$ mesons are identified by their semileptonic decays $D_s^- \to \phi e^- \bar{\nu}_e$ with $\phi \to K^+ K^-$ and $\bar{D}^0 \to K^+ e^- \bar{\nu}_e$, where the electron is used to tag the events and the missing energy due to the escaping neutrino is also used to suppress backgrounds. Since the neutrinos are undetectable, the D_s^- and $\bar{D}^0$ mesons cannot be directly identified by their invariant mass of the decay products. However, because of the two-body final states, they can be identified in the distribution of mass recoiling against the ρ^+ and $\bar{K}^{*0}$ in $\rho^+ \to \pi^+ \pi^0 (\pi^0 \to \gamma\gamma)$ and $\bar{K}^{*0} \to K^- \pi^+$ decays, respectively.

Charged tracks in BESIII are reconstructed from MDC hits. For each charged track, the polar angle must satisfy $|\cos\theta| < 0.93$, and it must pass within ± 20 cm from the interaction point in the beam direction and within ± 2 cm of the beam line in the plane perpendicular to the beam. The number of charged tracks is required to be four with zero net charge. The TOF and the specific energy loss dE/dx of a particle measured in the MDC are combined to calculate particle identification (ID) probabilities Prob(i), where $i(i = e/\pi/K/p)$ is the particle type. Prob(K) > Prob(π) and Prob(K) > Prob(p) are required for kaon candidates, while Prob(π) > Prob(e), Prob(π) > Prob(K) and Prob(π) > Prob(p) are required for pion candidates. For electron candidates, besides the particle identification requirement of Prob(e) > Prob(π) and Prob(e) > Prob(K), $E/cP > 0.8$ is also required, where E/cP is the ratio of the energy deposited in the EMC to the momentum reconstructed from the MDC. In addition, $|\cos\theta| < 0.8$ is required for electron candidates since the particle ID efficiencies between data and MC agree better in the barrel.

Photon candidates are reconstructed by clustering EMC crystal energies. Efficiency and energy resolution are improved by including energy deposits in nearby TOF counters. A photon candidate has to be more than 20° away from any charged track, and the minimum energy is 25 MeV for barrel showers ($|\cos\theta| < 0.80$) and 50 MeV for end cap showers ($0.86 < |\cos\theta| < 0.92$). An EMC timing requirement, i.e., $0 \le t \le 700$ ns, is used to suppress electronic noise and energy deposits in the EMC unrelated to the

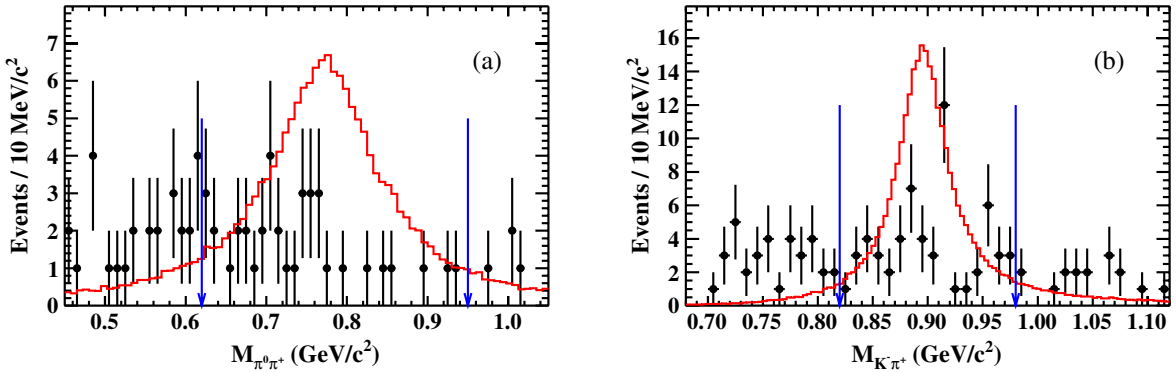

FIG. 2 (color online). The invariant mass distributions of resonance candidates for (a) ρ^+ from $J/\psi \to D_s^- \rho^+$, $\rho^+ \to \pi^+\pi^0(\pi^0 \to \gamma\gamma)$ and (b) $\bar{K}^{*0}$ from $J/\psi \to \bar{D}^0 \bar{K}^{*0}$, $\bar{K}^{*0} \to K^-\pi^+$. The requirements of $M_{\pi^0\pi^+} \in (0.62, 0.95)$ GeV/c^2 and $M_{K^-\pi^+} \in (0.82, 0.98)$ GeV/c^2 are shown in the figures by vertical arrows. The dots with error bars are data, while the histograms represent distributions of the arbitrarily normalized exclusive signal MC events.

events. Kinematic fits of pairs of photon candidates to the π^0 mass are performed. When there are more than two photons, all possible $\gamma\gamma$ combinations are considered, and the one yielding the smallest $\chi^2_{\gamma\gamma}$ is retained.

In the selection of $J/\psi \to D_s^- \rho^+ \to \phi e^- \bar{\nu}_e \pi^+ \pi^0 \to \gamma\gamma K^+ K^- \pi^+ e^- \bar{\nu}_e$, four charged track candidates and at least two photons are required. The invariant mass of K^+K^- for a ϕ candidate is required to satisfy $M_{K^+K^-} \in (1.01, 1.03)\,\mathrm{GeV}/c^2$. The invariant mass distribution of $\rho^+(\pi^0\pi^+)$ candidates is shown in Fig. 2(a) [21], and the requirement 0.62 GeV/c^2 $< M_{\pi^0\pi^+} <$ 0.95 GeV/c^2 is used to select ρ candidates. The $\chi^2_{\gamma\gamma}$ of the kinematic fit should be less than 200 for the π^0 candidates in this selection.

The missing four-momentum $(E_{\mathrm{miss}}, \vec{P}_{\mathrm{miss}})$, which represents the four-momentum of the missing neutrino, is determined from the difference between the net four-momentum of the J/ψ particle and the sum of the four-momenta of all detected particles in the event. The missing momentum (P_{miss}) distribution is shown in Fig. 3(a). P_{miss} is required to be larger than 0.1 GeV/c to reduce the backgrounds from J/ψ decays to final states with four charged particles and no missing particles but with e/π misidentification. Figure 4(a) shows the distribution of $U_{\mathrm{miss}} = E_{\mathrm{miss}} - cP_{\mathrm{miss}}$, and $|U_{\mathrm{miss}}|$ is required to be less than 0.05 GeV to reduce backgrounds such as $K^+K^-\pi^+\pi^-$ with multiple π^0 or γ in the final state, which were not rejected by prior criteria. After all selection criteria are applied, 11 events survive in the $(1.85, 2.10)$ GeV/c^2 mass region in the distribution of mass recoiling against the ρ^+, which is shown in Fig. 5(a). No accumulation of events in the signal region is found.

In the selection of $J/\psi \to \bar{D}^0 \bar{K}^{*0} \to K^+K^-\pi^+e^-\bar{\nu}_e$, there are only four charged tracks in the final state. To suppress backgrounds containing π^0s, kinematic fits to the π^0 mass are also performed if there are at least two photons in addition to the charged tracks. If there is a π^0 candidate with $\chi^2_{\gamma\gamma} < 20$, the event is vetoed. The $K^-\pi^+$ invariant mass distribution is shown in Fig. 2(b). To select $\bar{K}^{*0}$ candidates, the $K^-\pi^+$ invariant mass is required to satisfy $M_{K^-\pi^+} \in (0.82, 0.98)$ GeV/c^2. The $P_{\mathrm{miss}} > 0.1$ GeV/c and $|U_{\mathrm{miss}}| < 0.02$ GeV requirements are also used to suppress the backgrounds with e/π misidentification or multiphotons in the final states, and their distributions are

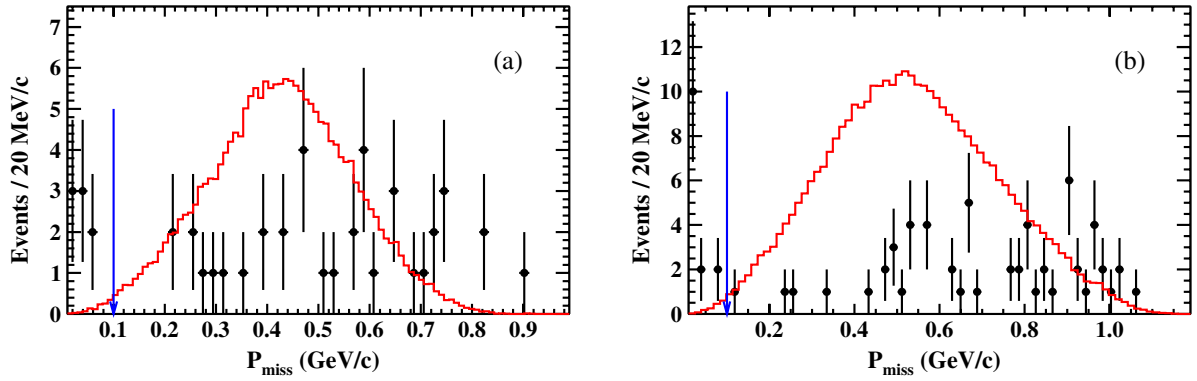

FIG. 3 (color online). P_{miss} distributions for the decay of (a) $J/\psi \to D_s^- \rho^+$ and (b) $J/\psi \to \bar{D}^0 \bar{K}^{*0}$. The requirement $P_{\mathrm{miss}} >$ 0.1 GeV/c is shown in the figures by vertical arrows. The dots with error bars are data, while the histograms represent distributions of the arbitrarily normalized exclusive signal MC events.

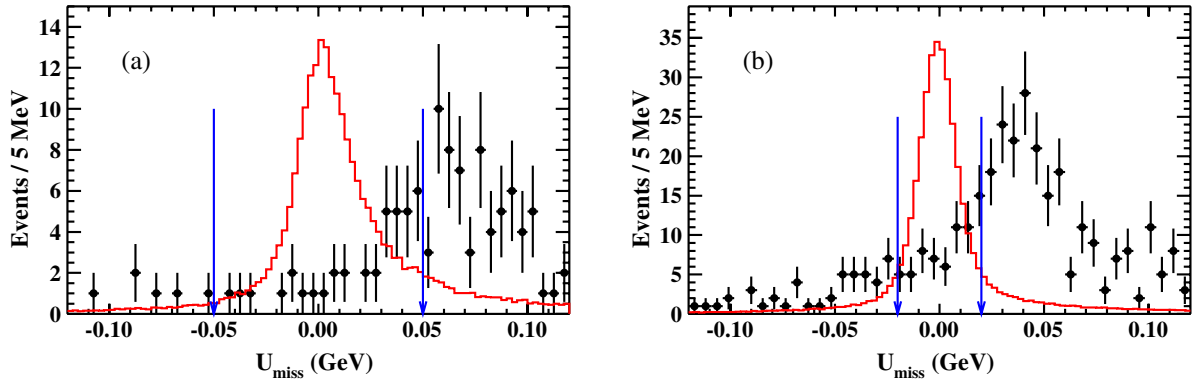

FIG. 4 (color online). $U_{\rm miss}$ distributions for the decay of (a) $J/\psi \to D_s^- \rho^+$ and (b) $J/\psi \to \bar{D}^0 \bar{K}^{*0}$. The requirements $|U_{\rm miss}| < 0.05$ GeV and $|U_{\rm miss}| < 0.02$ GeV are shown in the figures by vertical arrows. The dots with error bars are data, while the histograms represent distributions of the arbitrarily normalized exclusive signal MC events.

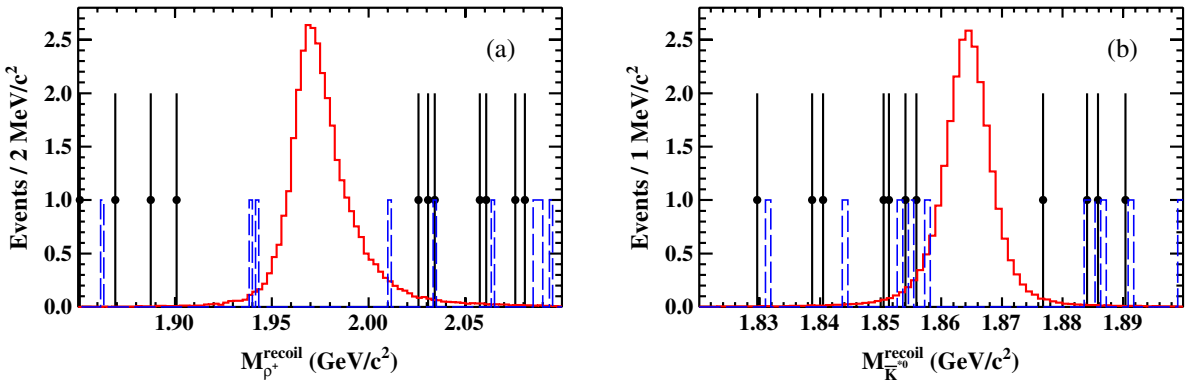

FIG. 5 (color online). Mass distributions recoiling against (a) ρ^+ from $J/\psi \to D_s^- \rho^+$ and (b) $\bar{K}^{*0}$ from $J/\psi \to \bar{D}^0 \bar{K}^{*0}$. Data are shown by dots with error bars. The solid histograms are the unnormalized MC-simulated signal events, while the dashed histograms are background distributions from selected inclusive MC events.

shown in Figs. 3(b) and 4(b), respectively. After all selection criteria are applied, 11 events survive in the $(1.82, 1.90)$ GeV/c^2 mass region in the distribution of mass recoiling against the $\bar{K}^{*0}$, which is shown in Fig. 5(b). No accumulation of events in the signal region is found.

MC simulations are used to determine mass resolutions and selection efficiencies and to study possible backgrounds. Six hundred thousand exclusive signal MC events are generated, and the selection efficiencies are determined to be $(7.79 \pm 0.04)\%$ and $(21.83 \pm 0.06)\%$ for $J/\psi \to D_s^- \rho^+$ and $J/\psi \to \bar{D}^0 \bar{K}^{*0}$, respectively. Two-hundred million inclusive J/ψ MC events are used to investigate possible backgrounds from J/ψ decays. For the decay $J/\psi \to D_s^- \rho^+$, 11 MC events pass the final selection criteria, and eight of them are due to e/π misidentification, where a pion is identified as an electron. For the remaining three events, two events are $\pi^0 \to \gamma e^+ e^-$, where an electron is identified as a pion, and the other is $\pi^+ \to \mu^+ \nu_\mu$, $\mu^+ \to e^+ \nu_e \bar{\nu}_\mu$. For the decay $J/\psi \to \bar{D}^0 \bar{K}^{*0}$, ten MC events pass the final selection criteria. Seven events are due to e/π misidentification. Two events are from $\pi^0 \to \gamma e^+ e^-$, and the other event is from $\pi^+ \to \mu^+ \nu_\mu, \mu^+ \to e^+ \nu_e \bar{\nu}_\mu$. From the inclusive MC study, both the number of surviving background events and their distributions shown as the dashed histogram in Fig. 5 are consistent with data.

Sideband events are also used to estimate the background. Here, the backgrounds contributions are estimated using $U_{\rm miss}$ sidebands, defined as $|U_{\rm miss}| \in (0.05, 0.10)$ GeV and $|U_{\rm miss}| \in (0.08, 0.10)$ GeV for $J/\psi \to D_s^- \rho^+$ and $J/\psi \to \bar{D}^0 \bar{K}^{*0}$, respectively. There are 15 and 9 sideband events surviving in the D_s^- and $\bar{D}^0$ mass region. The number of surviving background events and their distributions from sideband data are also consistent with data.

IV. SYSTEMATIC ERRORS

In this analysis, the systematic errors in the determination of the branching fraction upper limits mainly come from the following sources:

(i) MDC tracking: The MDC tracking efficiency is studied in clean channels like $J/\psi \to \rho\pi \to \pi^+\pi^-\pi^0$, $J/\psi \to p\bar{p}\pi^+\pi^-$, and $J/\psi \to K_S^0 K^+ \pi^-$ samples [22]. It is found that the MC simulation agrees with data within 1.0% for each charged track. Therefore,

TABLE I. Summary of systematic errors (%).

Sources	$J/\psi \to D_s^- \rho^+$	$J/\psi \to \bar{D}^0 \bar{K}^{*0}$
MDC tracking	4.0	4.0
Photon detection	2.0	2.0
Particle ID	4.0	4.0
π^0 kinematic fit	0.2	1.0
ϕ mass window	1.0	...
ρ^+ mass window	1.0	...
$\bar{K}^{*0}$ mass window	...	0.5
$U_{\rm miss}$ window	1.0	4.0
Intermediate decays	5.7	1.1
MC statistics	0.5	0.3
Number of J/ψ events	1.2	1.2
Total	8.6	7.5

4.0% is taken as the systematic error on the tracking efficiency for the two channels analyzed with four charged tracks in the final states.

(ii) Photon detection: The photon detection efficiency is studied from $J/\psi \to \rho^0\pi^0$ and photon conversion via $e^+e^- \to \gamma\gamma$ [23]. The difference between the detection efficiencies of data and MC simulation is 1.0% for each photon.

(iii) Particle ID: The particle ID efficiencies of electrons, pions, and kaons are studied with samples of radiative Bhabha events, $J/\psi \to p\bar{p}\pi^+\pi^-$, and $J/\psi \to K_S^0 K^+\pi^-$, respectively [22]. The kaon, pion, and electron particle ID efficiencies for data agree with MC simulation within 1% for each charged particle, and 4% is taken as the systematic error from this source.

(iv) π^0 kinematic fit: To estimate the systematic error from the π^0 kinematic fit in the analysis of $J/\psi \to D_s^-\rho^+$, a clean π^0 sample is selected from $J/\psi \to \rho^+\pi^-(\rho^+ \to \pi^0\pi^+)$ without the kinematic fit. Events with two oppositely charged tracks identified as pions and two photons are selected. Further, the π^- momentum is required to be in the range of $P_{\pi^-} \in (1.4, 1.5)$ GeV/c, and the $\pi^+\pi^-\pi^0$ invariant mass is required to be in the J/ψ mass region $|M_{\pi^+\pi^-\pi 0} - M_{J/\psi}| < 0.05$ GeV/c^2. In addition, E/cP is required to be less than 0.8 to remove Bhabha events.

After the above selection, a same π^0 kinematic fit as the one in the selection of $J/\psi \to D_s^-\rho^+$ is done on the candidates. The same analysis is also performed with MC events. The efficiency difference between data and MC simulation due to the π^0 kinematic fit with $\chi^2 < 200$ is 0.2%, which is regarded as the systematic error.

Applying a similar method, the efficiency difference of the π^0 kinematic fit used for vetoing events in the decay $J/\psi \to \bar{D}^0\bar{K}^{*0}$ is determined to be 1.0% using a sample of $J/\psi \to \bar{K}^{*0}K_S^0(\bar{K}^{*0} \to K^-\pi^+, K_S^0 \to \pi^+\pi^-)$ events.

(v) Mass window requirements: The systematic errors of the mass window requirements are due to the difference in mass resolution between MC simulation and data and are estimated from some control samples, which are selected without the mass window requirements. The uncertainty is obtained by comparing the efficiencies of mass window requirements between data and MC events. The uncertainties of ϕ, ρ^+, and $\bar{K}^{*0}$ mass window requirements are 1.0%, 1.0%, 0.5% using samples of $J/\psi \to \gamma\phi\phi(\phi \to K^+K^-)$, $J/\psi \to \rho^+\pi^-$, and $J/\psi \to \bar{K}^{*0}K_S^0$, respectively.

(vi) $U_{\rm miss}$ requirement: The systematic error of the $U_{\rm miss}$ window requirement is due to the mass resolution difference between MC simulation and data. Using a similar method as that used for the mass window requirement, the uncertainties of the $U_{\rm miss}$ requirements are 1.0% for $J/\psi \to D_s^-\rho^+$ and 4.0% for $J/\psi \to \bar{D}^0\bar{K}^{*0}$, which are different for the two channels since the $U_{\rm miss}$ requirements are different in these two channels.

(vii) Intermediate decays: The errors on the intermediate-decay branching fractions of $D_s^- \to \phi e^-\bar{\nu}_e$, $\phi \to K^+K^-$, $\rho^+ \to \pi^+\pi^0$, $\pi^0 \to \gamma\gamma$, and $\bar{D}^0 \to K^+e^-\bar{\nu}_e$, $\bar{K}^{*0} \to K^-\pi^+$ are taken from world average values [19], and by adding them in quadrature, 5.7% and 1.1% are the errors for $J/\psi \to D_s^-\rho^+$ and $J/\psi \to \bar{D}^0\bar{K}^{*0}$, respectively.

The systematic error contributions studied above, the error due to the uncertainty on the number of J/ψ events [13], and MC statistics are all summarized in Table I. The total systematic errors are obtained by summing them in quadrature, assuming that they are independent.

V. RESULTS

No excess of $J/\psi \to D_s^-\rho^+$ or $J/\psi \to \bar{D}^0\bar{K}^{*0}$ events above background is observed. The upper limits on the

TABLE II. Numbers used in the calculation of upper limits on the branching fractions of $J/\psi \to D_s^-\rho^+$ and $J/\psi \to \bar{D}^0\bar{K}^{*0}$. ε is the detection efficiency. $\mathcal{B}_{\rm inter}$ is the intermediate branching fraction. $\sigma^{\rm sys}$ is the systematic error. $N_{\rm UL}$ is the upper limit of the number of observed events at the 90% C.L. $\mathcal{B}$ is the upper limit at the 90% C.L. on the branching fraction.

Decay mode	Intermediate decay	ε	$\mathcal{B}_{\rm inter}$	$\sigma^{\rm sys}$	$N_{\rm UL}$	$\mathcal{B}$ (90% C.L.)
$J/\psi \to D_s^-\rho^+$	$D_s^- \to \phi e^-\bar{\nu}_e$, $\phi \to K^+K^-$, $\rho^+ \to \pi^+\pi^0$, $\pi^0 \to \gamma\gamma$	7.79%	1.20%	8.6%	2.5	$< 1.3 \times 10^{-5}$
$J/\psi \to \bar{D}^0\bar{K}^{*0}$	$\bar{D}^0 \to K^+e^-\bar{\nu}_e$, $\bar{K}^{*0} \to K^-\pi^+$	21.83%	2.37%	7.5%	2.7	$< 2.5 \times 10^{-6}$

branching fractions of these decay modes are calculated using

$$\mathcal{B} < \frac{N_{\rm UL}}{N_{J/\psi}\varepsilon\mathcal{B}_{\rm inter}(1-\sigma^{\rm sys})}, \quad (1)$$

where $N_{\rm UL}$ is the upper limit of the number of observed events at the 90% C.L., $N_{J/\psi}$ is the number of J/ψ events, ε is the detection efficiency, $\mathcal{B}_{\rm inter}$ is the intermediate branching fraction, and $\sigma^{\rm sys}$ is the systematic error.

The upper limits for the observed number of events at the 90% C.L. are 2.5 for $J/\psi \to D_s^-\rho^+$ and 2.7 for $J/\psi \to \bar{D}^0\bar{K}^{*0}$ using a series of unbinned extended maximum likelihood fits. In the fit, the recoil mass distributions of data, shown in Fig. 5, are fitted with a probability density function (p.d.f.) signal shape determined from MC simulations, and the background is represented by a second-order Chebychev polynomial. The likelihood distribution, determined by varying the number of signal events from zero to a large number, is taken as the p.d.f. $N_{\rm UL}$ is the number of events corresponding to 90% of the integral of the p.d.f. The fit-related uncertainties are estimated by using different fit ranges and different orders of the background polynomial, and $N_{\rm UL}$ is taken as maximum value among the variations. All numbers used in the calculations of the upper limits on the branching fractions are shown in Table II.

In summary, a search for the weak decays of $J/\psi \to D_s^-\rho^+$ and $J/\psi \to \bar{D}^0\bar{K}^{*0}$ has been performed using a sample of $(225.3 \pm 2.8) \times 10^6$ J/ψ events collected at the BESIII detector. No evident signal is observed, and upper limits at the 90% C.L. are set on the branching fractions, $\mathcal{B}(J/\psi \to D_s^-\rho^+) < 1.3 \times 10^{-5}$ and $\mathcal{B}(J/\psi \to \bar{D}^0\bar{K}^{*0}) < 2.5 \times 10^{-6}$, for the first time. These upper limits exclude new physics predictions which allow flavor-changing processes to occur with branching fractions around 10^{-5} but are still consistent with the predictions of the SM.

ACKNOWLEDGMENTS

The BESIII collaboration thanks the staff of BEPCII and the computing center for their strong support. This work is supported in part by the Ministry of Science and Technology of China under Contract No. 2009CB825200; the Joint Funds of the National Natural Science Foundation of China under Contracts No. 11079008, No. 11179007, No. 11179014, and No. U1332201; the National Natural Science Foundation of China (NSFC) under Contracts No. 10625524, No. 10821063, No. 10825524, No. 10835001, No. 10935007, No. 11005122, No. 11125525, No. 11235011, and No. 11275210; the Chinese Academy of Sciences (CAS) Large-Scale Scientific Facility Program; the CAS under Contracts No. KJCX2-YW-N29 and No. KJCX2-YW-N45; the 100 Talents Program of CAS; the German Research Foundation DFG under Contract No. Collaborative Research Center CRC-1044; the Istituto Nazionale di Fisica Nucleare, Italy; the Ministry of Development of Turkey under Contract No. DPT2006K-120470; the U.S. Department of Energy under Contracts No. DE-FG02-04ER41291, No. DE-FG02-05ER41374, No. DE-FG02-94ER40823, and No. DESC0010118; the U.S. National Science Foundation; the University of Groningen (RuG) and the Helmholtzzentrum fuer Schwerionenforschung GmbH (GSI), Darmstadt; and the WCU Program of National Research Foundation of Korea under Contract No. R32-2008-000-10155-0.

[1] M. A. Sanchis, Z. Phys. C **62**, 271 (1994).
[2] A. Datta, P. J. O'Donnell, S. Pakvasa, and X. Zhang, Phys. Rev. D **60**, 014011 (1999).
[3] X. Zhang, High Energy Phys. Nucl. Phys. **25**, 461 (2001).
[4] The charge conjugate states are implicitly included throughout this paper.
[5] M. Ablikim *et al.* (BES Collaboration), Phys. Lett. B **639**, 418 (2006).
[6] M. Ablikim *et al.* (BES Collaboration), Phys. Lett. B **663**, 297 (2008).
[7] Y. M. Wang, H. Zou, Z. T. Wei, X. Q. Li, and C. D. Lü, Eur. Phys. J. C **55**, 607 (2008).
[8] Y. L. Shen and Y. M. Wang, Phys. Rev. D **78**, 074012 (2008).
[9] H. B. Li and S. H. Zhu, Chin. Phys. C **36**, 932 (2012).
[10] R. C. Verma, A. N. Kamal, and A. Czarnecki, Phys. Lett. B **252**, 690 (1990).
[11] R. Dhir, R. C. Verma, and A. Sharma, Adv. High Energy Phys. **2013**, 706543 (2013).
[12] K. K. Sharma and R. C. Verma, Int. J. Mod. Phys. A **14**, 937 (1999).
[13] M. Ablikim *et al.* (BESIII Collaboration), Chin. Phys. C **36**, 915 (2012).
[14] M. Ablikim *et al.* (BESIII Collaboration), Nucl. Instrum. Methods Phys. Res., Sect. A **614**, 345 (2010).
[15] J. Z. Bai *et al.* (BES Collaboration), Nucl. Instrum. Methods Phys. Res., Sect. A **344**, 319 (1994); (**458**,627 (2001).
[16] S. Agostinelli *et al.* (GEANT4 Collaboration), Nucl. Instrum. Methods Phys. Res., Sect. A **506**, 250 (2003).

[17] S. Jadach, B. F. L. Ward, and Z. Was, Comput. Phys. Commun. **130**, 260 (2000); Phys. Rev. D **63**, 113009 (2001).
[18] D. J. Lange, Nucl. Instrum. Methods Phys. Res., Sect. A **462**, 152 (2001).
[19] J. Beringer *et al.* (Particle Data Group), Phys. Rev. D **86**, 010001 (2012).
[20] J. C. Chen, G. S. Huang, X. R. Qi, D. H. Zhang, and Y. S. Zhu, Phys. Rev. D **62**, 034003 (2000).
[21] Throughout this paper, the plot shows the distribution with requirements applied to all other variables except the one shown on it.
[22] M. Ablikim *et al.* (BESIII Collaboration), Phys. Rev. D **83**, 112005 (2011).
[23] M. Ablikim *et al.* (BESIII Collaboration), Phys. Rev. D **81**, 052005 (2010).